TEMPERATURE INDUCED DISSOLUTION OR PRECIPITATION IN GEOTHERMAL RESERVOIRS AND THEIR EFFECTS ON PRESSURE TRANSIENT ANALYSIS

Serhat AKIN

Middle East Technical University
Petroleum and Natural Gas Engineering Dept, Dumlupinar Bulvari No:1
Ankara, 06531, Turkey
e-mail: serhat@metu.edu.tr

ABSTRACT

Under in situ conditions, geothermal reservoir fluids are in equilibrium with co-existing mineral phases or close to saturation. When cool water is re-injected into the hot reservoir or for long production periods the equilibrium between fluid and reactive minerals is disturbed. This may result in temperature induced dissolution or precipitation. Predicting the permeability changes caused by chemical reactions in such reservoirs over the entire period of operation one requires understanding of the complex interactions of the involved processes, namely flow, heat transfer, transport of dissolved species, and chemical reactions. A chemical reaction model coupled with a relationship between porosity and permeability was used to simulate pressure transient tests conducted in such reservoirs. Several different cases were generated by changing deposition and dissolution rates. The pressure transient analyses showed marked differences in early time region in the form of changing wellbore storage.
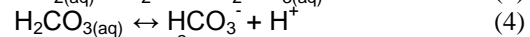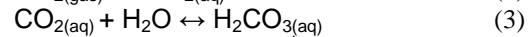
INTRODUCTION

One of the most common production problems in geothermal fields is calcite (calcium carbonate) scale deposition. Calcite blockages formed in near wellbore region or in the wellbore decrease significantly the output of the production well. Calcite scaling is experienced in almost all the geothermal fields around the world, i.e. in the Dixie Valley geothermal field, Nevada (Benoit, 1989), in Ohaaki geothermal field, New Zealand (Clotworthy et al., 1995 and Nogara, 1999), in Seltjarnarnes geothermal field, Iceland (Kristmansdottir et al., 1995) and in Coso geothermal area in California (Evanoff et al., 1995). In extreme cases, most of the production wells and surface facilities may get blocked by calcite scale and serious generation losses could be encountered, i.e. Kizildere geothermal field in Turkey (Durak et al., 1993). In some cases calcite deposition, together with anhydrite (calcium sulphate) in the wellbores were also reported, i.e. Oguni geothermal field in Kyushu, Japan (Todaka et al., 1995). Likewise in Sumikawa field, Akita, Japan, for example, CO_2-rich groundwaters are thought to have reacted with reservoir rocks to form a carbonate and kaolinite alteration assemblage (Ueda et al., 2001).
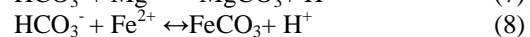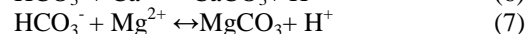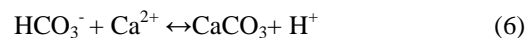
Calcite may form from hydrolysis (involving replacement of calcium alumino silicates), boiling of geothermal fluids (from fluids having high dissolved carbon dioxide concentrations and in the absence of mineral pH buffer) and heating of cooler peripheral geothermal fluids (Simmons and Christenson, 1993). In a boiling environment, calcite precipitates in open spaces upon loss of carbon dioxide with the carbonate species mostly controlling the pH and is described by the reaction (Izgec et al, 2008):

$$H_2O + CO_2 + CaCO_3 \leftrightarrow Ca(HCO_3)_2 \qquad (1)$$
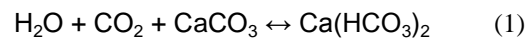
In general, CO_2 dissolves in water and generates a week carbonic acid, which subsequently dissociates into HCO3- and CO3- according to reaction steps given as:

$$CO_{2(gas)} \leftrightarrow CO_{2(aq)} \qquad (2)$$
$$CO_{2(aq)} + H_2O \leftrightarrow H_2CO_{3(aq)} \qquad (3)$$
$$H_2CO_{3(aq)} \leftrightarrow HCO_3^- + H^+ \qquad (4)$$
$$HCO_3^- \leftrightarrow CO_3^{2-} + H^+ \qquad (5)$$

The dissolved bicarbonate species react with divalent cations to precipitate carbonate minerals. Formation of Ca, Mg, and Fe(II) carbonates are expected to be the primary means by which CO_2 is immobilized (Gunter et al., 1997).

$$HCO_3^- + Ca^{2+} \leftrightarrow CaCO_3 + H^+ \qquad (6)$$
$$HCO_3^- + Mg^{2+} \leftrightarrow MgCO_3 + H^+ \qquad (7)$$
$$HCO_3^- + Fe^{2+} \leftrightarrow FeCO_3 + H^+ \qquad (8)$$

Mechanisms with which a precipitate reduce permeability include deposition of the carbonate

particles precipitated from the saturated solution on the pore walls due to attractive forces between the particles and the surfaces of the pores, individual particles blocking pore throats, and several particles bridging across a pore throat (Pruess and Xu, 2001). In a carbonate formation major cause of reduction in rock properties is precipitation of $Ca(HCO_3)_2$ and $NaCl$. Pressure drop through the flow paths affects the precipitation rate, thus leads to variations in rock properties by changing the solubility of substances. Assuming there is Darcian flow in the porous media, it can be said that there is a linear relationship between the pressure drop and the axial distance in the direction of flow. Considering this relationship and solute transport concept, it should be expected that permeability increases in near well bore region and then gradually decreases through to flow direction (Omole and Osaba, 1983). In the case of multiphase flow and/or heterogeneous and fractured formations dramatic deviations from the linear pressure decrease are reported (Matthai and Belayneh, 2004). This in turn may affect the permeability alteration trends. It is previously reported that permeability decline caused by only calcite deposition in the porous bed can reach to 90% of the initial permeability, depending on solution composition, initial permeability, temperature, and flow rate and solution injection period (Moghadasi et al., 2005). On the other hand some researchers (Omole and Osaba, 1983) reported increase in the permeability of dolomite cores by 3.5 to 5% after similar CO_2 treatments while reduction in permeability was observed for other experiments. Those results suggest that the process strongly depends on the distribution of the rock minerals.

From the calcite dissolution equations (the $CaCO_3$-CO_2-H_2O system) it is quite clear that removal of CO_2 to a steam phase during flashing leads to calcite supersaturation even though the accompanying temperature drop itself leads to calcite saturation increase. Since most reservoir fluids are close to saturation with calcite, carbonate scaling inside the well above the bubble point depth and inside production casing is a possibility for all geothermal wells. The solubility of calcium carbonate minerals in aqueous solution at any particular temperature increases with increasing partial pressure of CO_2. Boiling leads to strong reduction in CO_2 partial pressure due to effective transfer of CO_2 into the steam phase. The presence of other gases in the geothermal fluid, especially if less soluble in water then CO_2 will enhance degassing of the CO_2 during boiling.

NUMERICAL MODELING

Main Features

CMG's STARS (CMG, 2003) compositional advanced processes and thermal finite difference reservoir simulator is capable of simulating many types of chemical additive processes such as surfactant and polymer injection, using cartesian or cylindrical grid and porosity models (single porosity or double porosity) in both laboratory and field scale. STARS is previously used to simulate several processes including CO_2 injection into coal bed methane reservoirs (Law et al., 2001), modeling phase behavior including the effect of pressure and temperature on asphaltene precipitation during primary production (Kohse et al., 2000) and fully implicit thermal simulation for multi component fluid flows (Siu et al., 1990). Law et al. (2001) stated that the predicted CH_4 production rates and compositions in the produced gas streams predictions by STARS and ECLIPSE were in general agreement for pure CO_2 injection into a coal bed methane reservoir. This indicates that STARS has a very similar performance even though it uses a very different modeling approach compared to ECLIPSE.

One conservation equation for each chemical component for which a separate accounting is desired, and two separate phases (water and gas) along with equations describing phase equilibrium between phases are used to model injection of CO_2. There exists a set of these equations for each region of interest, which is usually a discretized grid block. Lastly, there is an equation describing the operating condition of each injection and production well. An implicit time weighting scheme is used for the individual components of the model consisting of flow, transport, and geochemical reaction. A fully implicit approach, which simultaneously solves the transport and the reaction equations was used. No flow boundary conditions are used. CO_2 was defined as real gas and its solubility in water is taken to be proportional to CO_2 partial pressures at pressures of a few bars, but increases only very weakly with pressure beyond 100 bars (Spycher et al., 2003). A Henry's law formulation with fugacity correction was used. Supercritical dilute aqueous CO_2 thermodynamical properties adapted from Sengers et al (1992) are input in a tabular fashion. Water viscosity and density is taken to be function of temperature and salinity only. The dissolution and deposition reactions given by Eqn. 1 through 5 are implemented and treated separately. The reaction model's heterogeneous mass transfer (source and sink) terms were applied to the non-equilibrium capture and release of calcite particles as well as salt particles by the porous rock. These particles captured by the porous medium can cause permeability

reductions (blockage) in a manner similar to equilibrium mass transfer to the rock (adsorption). The reaction source/sink term is given as:

$$V\sum_{k=1}^{nr}\left(s_{ki}^{'}-s_{ki}\right)\bullet rk \qquad (9)$$

Where ski and s'ki represent the reactant and product stoichiometric coefficients of reaction k. Eqn. 9 proceeds at the rate of rk moles per day per reservoir volume. This relationship has one degree of freedom, which is a proportionality factor. The quantities ski and s'ki can be multiplied by an arbitrary factor "a", but rk must be divided by "a" so that the source/sink terms remain. Usually the factor "a" is chosen such that ski = 1 for the main reacting component. The kinetic model determines the speed of reaction rk. The general expression is given by:

$$rk=r_{rk}.\exp(\frac{-E_{ak}}{RT}).\prod_{i=1}^{nc}C_{i} \qquad (10)$$

Where r_{rk} is reaction rate constant that specifies the frequency of the reaction, E_{ak} is the activation energy E_{ak} that determines the temperature dependence of reaction rate, r_k. While the enthalpies of reaction can be characterized between well defined limits and can even be calculated from first principles, the observed activation energies can vary dramatically. This is because certain components in the rock surface may act as catalysts. The concentration factor for reacting component i is given as follows:

$$C_{i}=\varphi_{f}.\rho_{j}.s_{j}.x_{ji} \qquad (11)$$

Where j is the phase in which component i is reacting, and x_{ji} represents water or gas mole fractions, φ_{f} is fluid porosity, ρ_{j} is density, s_j is saturation. Concentration factor for the solid component is given by

$$C_{i}=\varphi_{v}c_{i} \qquad (12)$$

Where φ_{v} is void porosity (ratio of void volume to gross volume) and c_i is the concentration of component i in void volume. The void porosity can be occupied by fluids (represented by fluid porosity, φ_f) and the deposited calcite particles (represented by solid porosity, φ_s). Fluid porosity and void porosity is related with the following relationship.

$$\varphi_{f}=\varphi_{v}=\left[1-F_{fluid}-\sum_{i}\left(\frac{c_{i}}{\rho_{si}}\right)\right] \qquad (13)$$

Where F_{fluid} is the fraction of void volume occupied by fluid components. It then requires that the permeability depends upon reaction rate constants, to account for the changes in capture efficiency as the calcite particle size to pore throat size ratio changes. To specify the dependence of permeability on chemical reactions and non-equilibrium mass transfer

an effective permeability reaction rate scaling factor table (i.e. Table 2) was used. Once porosity as a function of time is calculated permeability is adjusted accordingly. Thus, permeability change was controlled by reaction frequencies (1/min-kPa) of the dissolution and deposition reactions and Kozeny-Carman coefficient (c) given by Eqn. 14 (CMG, 2003).

$$k_{f}=k_{0}\left(\frac{\phi}{\phi_{0}}\right)^{c}\left(\frac{1-\phi_{0}}{1-\phi}\right)^{2} \qquad (14)$$

The rate of propagation of in situ created calcite particles are strongly affected by their interaction with the rock matrix. These interactions can be chemical (e.g. ion exchange) or mechanical (e.g. blockage) or some combination of mechanisms. The capture levels can depend on fluid concentrations, temperature and rock type (e.g. permeability). A phenomenological description of these phenomena, wherein a set of constant temperature adsorption isotherms (adsorption level as a function of fluid composition) are input, is adapted. These isotherms can be either in tabular form or in terms of the well known Langmuir isotherm correlation.

$$AD=\frac{A.z}{1+Bz} \qquad (15)$$

Where z is some fluid component composition, A and B are generally temperature dependent Langmuir constants. The maximum adsorption level associated with this formula is A/B. Permeability alteration often accompanies adsorption (especially if adsorption is of mechanical, blockage type). The simulator accounts for this via region dependent resistance factors (RRF) which allow correlation of local permeability with local adsorption levels. It is assumed that only single-phase flow paths are altered. Thus for example, the gas phase permeability reduction factor is defined as

$$RKG=1+(RRF-1)*AD/ADMAXT \qquad (16)$$

RKG varies between 1.0 and a maximum of RRF as adsorption level increases. The mobility of the gas phase is divided by RKG, thus accounting for blockage. Ideally, not only the adsorption maximum but the rate of increase of adsorption with fluid composition should be known in order to fit the two Langmuir parameters A and B. If this is not reported, as is often the case, one must use the fluid composition at the adsorption maximum to indirectly determine this second factor.

For a typical problem cumulative mass balance errors at the ending time were less than 1% for all components. In order to achieve this level of accuracy and to prevent large material balance errors due to insufficient accuracy of iterative matrix solution, a precision parameter that is the ratio by

which the mean equation residual must be reduced from its initial value before the solution is accepted was used. When used with an automatic time step cutting control algorithm this method ensured accurate solutions with 10 to 15 Newton cycles per time step. As the size of a problem increases, the relative amount of time spent in the various STARS component routines will change. The time spent in the EOS routine increases roughly linearly with the size of the problem (number of equations solved). Solution time of the linear equations increases roughly proportional to the problem size raised to an exponent of about 1.4–1.6 (using iterative solvers) or 3 for direct solvers. In typical, large STARS runs, on the order of 60% of the execution time is spent in the linear equation solver and a further 30% is spent setting up the Jacobian matrices.

METHOD

In order to study the effect of temperature induced dissolution or precipitation in geothermal reservoirs and their effects on pressure transient analysis several numerical experiments were constructed. In these experiments a quarter of 5-spot pattern is considered using 66 blocks. One production well operated at a constant rate 320 m^3/day and operating constraint of 500 kPa drained the fractured reservoir. The formulation used to represent fractured reservoir is MINC with 4 sub-matrices. Initial fracture and matrix permeabilities (x, y, and z directions) are $6x10^{-3}$ and $1x10^{-5}$ m^2 respectively. Power law relative permeabilities were used for the fracture. A constant porosity of 10% is used. The reaction rates, activation energies and enthalpies are reported in Izgec et al (2008). Other simulation parameters are reported in Pruess (1983). Buildup tests were conducted at three different times (397, 443 and 2430 days) to investigate the effect of cooling induced calcite precipitation.

Analyses of pressure transient tests were carried out in a systematic manner using a commercial well test analysis package (Kappa's Ecrin). The first step consisted of conventional semi-log and log-log analysis. Initial parameter estimates for several reservoir parameters like permeability were obtained at this stage. Then these estimates were fine-tuned using an automated history matching technique considering both the test history (i.e. considering all pressure points) and the analyzed buildup data only. The estimated parameters were accepted using 10% confidence intervals. During the estimation procedure two different types of wellbore conditions were considered: constant wellbore storage and skin, changing storage and skin. For both analyses a double porosity reservoir model was considered.

RESULTS

From the aforementioned discussion, critical simulation parameters can be summarized as follows:

1.   Dissolution and deposition reaction frequencies.
2.   Kozeny-Carman coefficient
3.   Reaction rate scaling factor
4.   Blockage effect of particles

Several simulations (Table 1) were conducted to study the effects of these parameters. Common to all runs it has been observed the order of permeability change depended on the magnitudes of dissolution and deposition reaction frequencies and reaction rate scaling factor. Fig 1 shows pressure and pressure derivative responses and the corresponding permeability distribution at three different times using the parameters given in Table 1. Solid lines represent the matches obtained using the aforementioned well test model. Although the permeability is decreasing near the producing well, the pressure and its derivative response are practically the same for 1.09 and 1.21 years. The derivative response is smooth and the permeability estimates obtained during the pressure buildups are practically the same. On the other the pressure buildup conducted at 6.65 years has a significantly different pressure derivative curve such that although the pressure derivative magnitude is comparable to those obtained earlier it's clearly much noisier (i.e. it doesn't have a smooth response). Applying smoothing does not help improving the pressure derivative noise. The permeability distribution shows that the dissolution-deposition affected region extends to a much larger area compared to those obtained with earlier buildup analyses. The estimated permeability reduced from 0.744 md to 0.647 md and then to 0.00858 md for 1.09, 1.21 and 6.65 years respectively. The improvement applying all test data as constraint in estimating parameters did not changed the match. When a variable wellbore storage model was used the match improved and the estimated permeability increased to 0.0106 md. The confidence intervals obtained for such analyses were typically significantly larger than 10% which is the industry accepted standard.

Several sensitivity runs were conducted to study the extent of permeability change and the resulting estimation. The sensitivity values presented in Table 1 were used while keeping the other parameters constant. In one case the flow restriction due to calcite precipitation is significantly reduced (1000 times). This case practically showed that if the flow paths are large enough to transport calcite particles a small effect will be observed compared to other

cases. Increasing the dissolution and deposition reaction frequency affected the size of the calcite precipitated and thus permeability affected area. It has been observed that the most effective parameter regarding the change in permeability is the Kozeny-Carman coefficient together with flow restriction parameter. When a large coefficient with large flow restriction factor is coupled the permeability change was the largest. For such numerical exercises the scatter in pressure derivative was the largest leading to a large confidence interval.

Table 1. Simulation and sensitivity parameters

|	Base	Sensitivity
Fracture Permeability, micro m^2	6x10^{-3}	6x10^{-3}
Matrix Permeability, micro m^2	1x10^{-5}	1x10^{-5}
Fracture Porosity, ratio	0.1	0.1
Matrix Porosity, ratio	0.1	0.1
Dissolution reaction frequency	4000	40000
Activation Energy	53500	53500
Reaction Enthalpy	-22900	-22900
Deposition reaction frequency	12000	120000
Activation Energy	53500	53500
Reaction Enthalpy	42700	42700
Kozeny-Carman Coefficient	0.1	0.5, 2.5
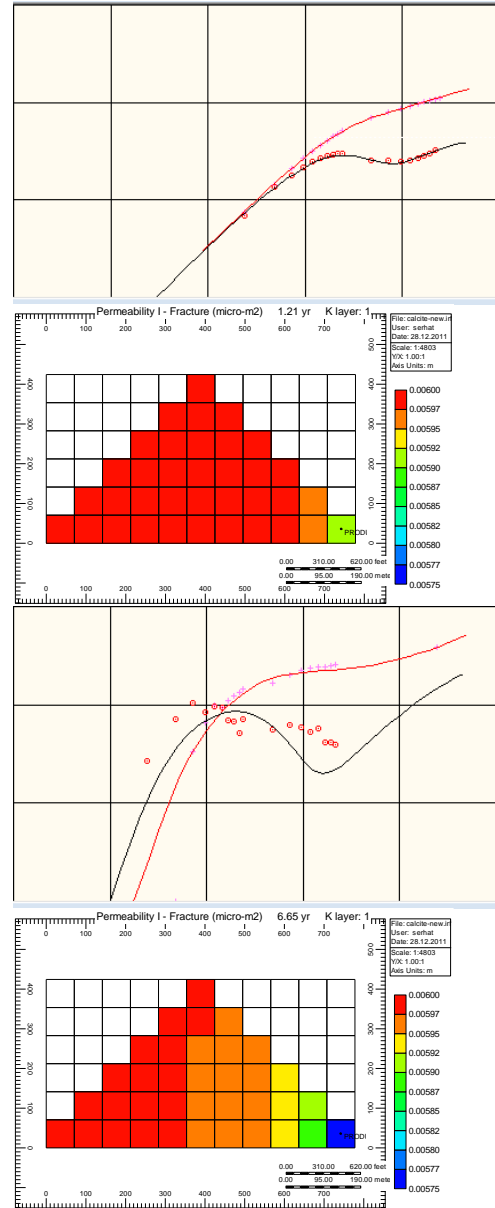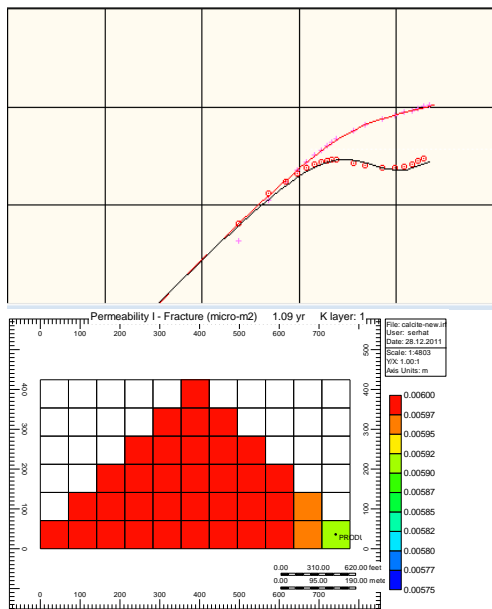
Figure 1: *Permeability change and corresponding pressure transient and derivative respond at differing times.*

DISCUSSION

Little information is currently available on the precipitation kinetics. Thus, precipitation rate laws only consider the neutral mechanism and, it is assumed that the parameters of the precipitation kinetics equal those of the dissolution ones. Moreover, some mineral precipitation reactions are inhibited in favor of others more probable at the PT conditions studied. Mineral reactions proceed under kinetic conditions with the values of the kinetic parameters used for the modeling are adapted from Palandri and Kharaka (2004) and Izgec et al (2008).

Further research regarding experimental data is required.

CONCLUSIONS

Effect of permeability changes caused by chemical reactions in geothermal reservoirs due to temperature induced dissolution or precipitation over the entire period of operation was studied using a numerical model. A chemical reaction model coupled with a relationship between porosity and permeability was used to simulate pressure transient tests conducted in such reservoirs. Several different cases were generated by changing deposition and dissolution reaction frequencies, Kozeny – Carman coefficient and reaction rate scaling factor. The pressure transient analyses showed marked differences in early time region in the form of changing wellbore storage. In all cases the larger the dissolution and deposition reaction rate frequencies the permeability changed more and the scatter in pressure derivative increased. Matching a unique analytical well test model was harder for such cases. It was not possible to obtain confidence intervals smaller than 10% in such cases. As the magnitude of deposition increased permeability underestimation become severe.

REFERENCES

Benoit, W. R. (1989). Carbonate scaling characteristics in Dixie Valley, Nevada geothermal wellbores. Geothermics, vol. 18, pp. 41-48.

Clotworthy, A. Lovelock, B and Carey, B. (1995). Operational history of the Ohaaki geothermal field, New Zealand. Proc. World Geothermal Congress, 1995, pp. 1797-1802.

Computer Modeling Group (CMG): 2003. CMG STARS User's Guide, Computer Modeling Group LTD., Calgary, Alberta, Canada.

Durak, S., Erkan, B. and Aksoy, N. (1993). Calcite removal from wellbores at Kizildere geothermal field, Turkey. Proc. 15th New Zealand Workshop, pp. 11-15.

Evanoff, J., Yeager, V., and Spielman, P. (1995). Stimulation and damage removal of calcium carbonate scaling in geothermal wells: A case study. Proc. World Geothermal Congress, 1995, pp. 2481-2486.

Gunter, W.D., Wiwchar, B., Perkins, E.H., 1997. Aquifer disposal of CO2-rich greenhouse gases: Extension of the time scale of experiment for CO2-sequestering reactions by geochemical modelling. Mineral. Petrol. 59, 121–140.

Izgec, O., Demiral, B., Bertin, H., and Akin, S.: "CO2 injection into Saline Carbonate Aquifer Formations II: Comparison of Numerical Simulations to Experiments" Transport in Porous Media. 73(1), 57-74, 2008.

Kohse, B. F., Nghiem, L. X., Maeda, H., Ohno, K.: 2000. Modelling Phase Behaviour Including the Effect of Pressure and Temperature on Asphaltene Precipitation. SPE Asia Pacific Oil and Gas Conference and Exhibition, 16-18 October, Brisbane, Australia, Paper SPE 64465.

Kristmannsdottir, H. Arnornonsson, H., Axelson, G., Olafsson, M., Hakanarson, S., Thorhallson, S. (1995). Monitoring of Iceland geothermal field during production. Proc. World Geothermal Congress, 1995, pp 1813-1817.

Law, D. H., Van der Meer, L. H. G., Gunter, W. D.: 2001. Comparison of Numerical Simulators for Greenhouse Gas Storage in Coalbeds, Part I: Pure Carbon Dioxide Injection. In Proc.: 1st Nat. Conf. Carbon Sequestration. Washington, DC.

Matthai, S.K., Belayneh, M.: 2004. Fluid flow partitioning between fractures and a permeable rock matrix. Geophysical Research Letters 31 (7): Art. No. L07602.

Moghadasi, J., Müller-Steinhagen, H., Jamialahmadi M., Sharif, A.: 2005. Model Study on the Kinetics of Oil Formation Damage Due to Salt Precipitation from Injection. Journal of Petroleum Science & Engineering, 46 (4): 299-299.

Nogara, J.B. (1999). Calcium carbonate scaling in geothermal wells at Ohaaki. Proc. 20th Annual PNOC-EDC Geothermal Conference, pp. 91-98.

Omole O., Osoba J.S.: 1983: Carbon Dioxide – Dolomite Rock Interaction During CO2 Flooding Process, in: 34th Annual Technical Meeting of the Petroleum Society of CIM, Canada.

Palandri, J. L. and Kharaka, Y. K. (2004), "A compilation of rate parameters of water-mineral interaction kinetics for application to geochemical modelling", U.S. Geological Survey Report 2004-1068

Pruess, K. Heat Transfer in Fractured Geothermal Reservoirs with Boiling, Water Resources, Research, 19 (1), 201-208, February 1983.

Pruess K., Xu T.: 2001, Numerical Modeling of Aquifer Disposal of CO2, in: SPE/EPA/DOE Exploration and Production Environmental Conference, San Antonio,Texas, SPE Paper 83695.

Satman, A., Ugur, Z., Onur, M.: "The Effect of Calcite Deposition on Geothermal Well Inflow Performance", Geothermics, June 1999, 4(1), 425-444.

Sengers, J. M. H. L., Harvey, A. H., Crovetto, R., Gallagher, J. S.: 1992. Standard States, Reference States and Finite-Concentration Effects in Near-Critical Mixtures with Applications to Aqueous-Solutions. Fluid Phase Equilibria 81 (1-2): 85-107.

Simmons, S. F. and Christenson, B. W. (1993). Towards a Unified Theory on Calcite Formation in Boiling Geothermal Systems. Proc.15th New Zealand Geothermal Workshop, pp. 145-148.

Siu, A.L., Rozon, B.J., Li, Y. K., Nghiem, L. X.: 1990. A Fully Implicit Thermal Wellbore Model for Multicomponent Fluid Flows. SPE California Regional Meeting, Bakersfield, April 5-7, SPE 18777.

Spycher, N., Pruess, K. and Ennis-King, J.: 2003. CO_2-H_2O Mixtures in the Geological Sequestration of CO_2. I. Assessment and Calculation of Mutual Solubilities from 12 to 100 °C and up to 600 bar, Geochim. Cosmochim. Acta, 67 (16), 3015-3031.

Todaka, N., Kawano, Y., Ishii, H. and Iwai, N. (1995). Prediction of Calcite Scaling at the Oguni Geothermal Field, Japan: Chemical Modeling Approach. Proc. World Geothermal Congress, 1995, pp. 2475-2480.

Ueda, A., Ajima, S., and Yamamoto, M.: Isotopic study of carbonate minerals from the Sumikawa geothermal area and its application to water movement, J. Geotherm. Res. Soc. Japan, 23, 181–196, 2001.